

**Energetics and nucleation of point defects in aluminum under extreme tensile hydrostatic stresses**

Mrinal Iyer and Vikram Gavini\*

*Department of Mechanical Engineering, University of Michigan, Ann Arbor, Michigan 48109, USA*

Tresa M. Pollock

*Materials Department, University of California, Santa Barbara, California 93106, USA*

(Received 29 September 2013; revised manuscript received 7 January 2014; published 28 January 2014)

Density functional theory calculations are employed to investigate the energetics of point defects—monovacancy, self-interstitials (tetrahedral, octahedral, and dumbbell), and Frenkel pairs—in aluminum under tensile hydrostatic stresses. Our study suggests that the defect core energy of a vacancy, which is governed solely by the electronic structure at the core, significantly depends on the macroscopic hydrostatic stress, and that this constitutes an important contribution to the formation enthalpy, especially in the regime of extreme tensile hydrostatic stresses. This finding is in contrast to widely used elastic formulations of point defects based on formation volume that ignore the defect core-energy contribution. The formation enthalpies of all point defects considered in the present study monotonically decrease with increasing tensile hydrostatic stress. Furthermore, we find that the formation enthalpies of vacancies and Frenkel pairs are negative beyond critical tensile hydrostatic stresses (9 GPa for vacancies and 12 GPa for Frenkel pairs), which suggests a spontaneous nucleation of these point defects and this has important implications to nucleation mechanisms leading to spall failure. In particular, the present findings suggest two possible defect nucleation mechanisms leading to spall failure: (i) a heterogeneous nucleation of vacancies from defect sources and (ii) a homogeneous nucleation of Frenkel pairs at higher hydrostatic stresses.

DOI: [10.1103/PhysRevB.89.014108](https://doi.org/10.1103/PhysRevB.89.014108)

PACS number(s): 61.72.jd, 61.72.jj, 61.72.jn, 71.15.Mb

**I. INTRODUCTION**

Point defects play an important role in the nucleation, evolution, and kinetics of larger defects, which in turn govern the macroscopic deformation and failure mechanisms observed in a wide range of metals. For instance, vacancies play a crucial role in dislocation motion [1–3], mediating diffusion of various species in crystalline solids [4,5], and point defects are also responsible for the hardening phenomenon observed in metals subject to irradiation [6–9]. Furthermore, recent studies suggest vacancy nucleation and coalescence as a possible mechanism leading to spall failure in metals subjected to shock loading [10]. The energetics of point defects under extreme tensile hydrostatic stresses experienced during shock loading is one of the central issues in understanding the nucleation mechanisms leading to spall failure in metals.

In order to elucidate this crucial role of point defects in the observed deformation and failure mechanisms in crystalline solids, many efforts have been focused towards understanding the energetics of point defects from electronic-structure calculations (cf., e.g., [11–17]). However, excepting a few recent studies [15,16,18,19], the majority of these electronic-structure studies are restricted to studying their energetics in macroscopically stress-free solids. The role of macroscopic stresses on the energetics of point defects, which is crucial in understanding deformation mechanisms in solids, is often accounted for by taking a recourse to elastic formulations based on formation volume or volume tensor [20,21]. Such formulations account for the interactions between the elastic fields produced by the defect and macroscopic stresses. However, these formulations ignore the

effect of macroscopic deformations on the defect core which is governed by quantum-mechanical interactions at the core.

In the present study, we conduct density functional theory calculations to investigate the influence of macroscopic hydrostatic stress on the energetics of point defects—monovacancy, self-interstitials (tetrahedral, octahedral, and dumbbell), and Frenkel pairs—and study the role of the defect core in determining their overall energetics. As discussed subsequently, the defect core energy of a vacancy significantly depends on the macroscopic hydrostatic stress in the regime of extreme tensile stresses, and this constitutes an important contribution to the formation enthalpy. These findings underscore the importance of accounting for the defect core energy in the energetics of point defects, especially in the regime of extreme tensile stresses that are present during spall failure in shocked metals. Furthermore, we find that the formation enthalpies of vacancies and Frenkel pairs become negative beyond critical hydrostatic stresses, which suggests a spontaneous nucleation of these defects beyond these critical hydrostatic stresses and provides new insights into the nucleation mechanisms leading to spall failure.

**II. COMPUTATIONAL METHODS**

The density functional theory calculations in the present study are performed using the ABINIT software [22,23] by employing the Perdew-Zunger-Ceperley-Alder (no spin polarization) local-density-approximation (LDA) [24] for the exchange and correlation functionals. The electron-ion interactions are treated using the projector-augmented wave (PAW) method [25] using the PAW projectors for aluminum available in ABINIT software [26]. A cubic computational domain with face-centered-cubic (fcc) lattice and a cell size corresponding to a 108-atom system is employed to compute

\*Corresponding author: vikramg@umich.edu

the defect energies. An energy cutoff of 400 eV is used for the plane-wave discretization of wave functions, and  $6 \times 6 \times 6$   $k$ -points mesh generated by the Monkhorst-Pack scheme [27] is used for the Brillouin zone integration. The discretization errors associated with the chosen plane-wave discretization and Brillouin zone sampling are found to be of the order of 0.01 eV in the computed defect energies. The internal atomic relaxations in the simulations are performed till the maximum force component on any atom is less than 2.5 meV/Å. The volume relaxations are performed until the hydrostatic stress on the simulation cell is within 0.03 GPa of the prescribed hydrostatic stress. We note that previous studies suggest that cell-size effects in the computed defect energies, even in the case of point defects, can be up to 0.05 eV for cell sizes corresponding to a few hundred atoms [28,29]. However, as will be evident from the results, the effect of macroscopic hydrostatic stress on the defect energies is much larger than the finite cell-size effects. Thus, using a 108-atom supercell for the computation of the defect energies does not affect the main findings of the present work.

### III. RESULTS AND DISCUSSION

In order to study the effect of macroscopic state of stress on the energetics of point defects, we begin by computing the formation enthalpy of a monovacancy in fcc aluminum as a function of the applied hydrostatic stress. In the present work we restrict our study to a hydrostatic state of stress as the energetics of point defects like vacancies and self-interstitials, which are dilatational centers, are primarily affected by the hydrostatic component of the stress tensor. Recent studies on the role of macroscopic deformations on the energetics of monovacancy and divacancies also suggest that the volumetric strain associated with any deformation—produced by the hydrostatic component of the stress tensor—is the dominant parameter influencing the energetics of these defects [16,18]. Furthermore, we restrict our study to tensile hydrostatic states of stress—a regime of interest in understanding the nucleation mechanisms leading to spall failure in metals. Since a hydrostatic state of stress is given by an isotropic tensor  $\sigma_{ij} = \sigma_0 \delta_{ij}$ , where  $\delta_{ij}$  denotes the Kronecker delta, it is characterized by the normal stress along any direction  $\sigma_0$ , which is a scalar quantity. We note that  $\sigma_0$  is negative of the bulk pressure on the material system. In the present work we considered hydrostatic stresses up to 12 GPa to compute the defect energetics. We note that the maximum hydrostatic stress which can be supported by fcc aluminum is determined to be 12.95 GPa from the computed equation of state which is shown in Fig. 1.

The formation enthalpy of a monovacancy at a given macroscopic hydrostatic stress is computed as

$$H_f^v(\sigma_0) = H(N-1, 1v, \sigma_0) - \frac{N-1}{N} H(N, 0, \sigma_0), \quad (1)$$

where  $H(N-1, 1v, \sigma_0)$  denotes the enthalpy of a system comprising of  $N-1$  atoms and one vacancy ( $N$  corresponds to 108 atoms in the present study) computed at an applied hydrostatic stress  $\sigma_0$ , and  $H(N, 0, \sigma_0)$  denotes the enthalpy of a perfect crystal containing  $N$  atoms at the same stress state. We note that, here and subsequently, the volume relaxations of the

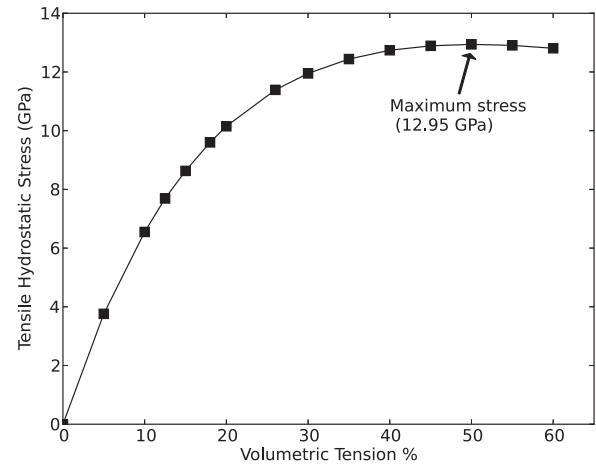


FIG. 1. Computed equation of state for aluminum.

simulation cells containing the defect and the perfect crystal are performed independently to achieve the target hydrostatic stress  $\sigma_0$ . The computed vacancy formation enthalpy as a function of macroscopic hydrostatic stress is shown in Fig. 2. Our results suggest that the monovacancy formation enthalpy is significantly influenced by the state of hydrostatic stress, where the formation enthalpy changes from 0.7 eV at no applied stress to  $-0.17$  eV at a hydrostatic stress of 10.15 GPa.

Prior calculations have attempted to account for this significant dependence of formation enthalpy on mechanical stresses by resorting to elastic formulations using formation volume [20] and volume tensors [21]. Such formulations describe the elastic interactions between the elastic fields produced by the defect and the macroscopic stresses. However, these formulations do not account for changes in the defect core energy due to changes in the electronic structure at the defect core resulting from macroscopic deformations. In particular, we note that the formation enthalpy of a defect at a given hydrostatic stress is related to the formation energy at the same stress by  $H_f(\sigma_0) = E_f(\sigma_0) - \sigma_0 V_f(\sigma_0)$ , where  $V_f$  denotes the defect formation volume—the excess volume due to the presence of the defect, measured with respect to a perfect crystal containing the same number of atoms at the same stress

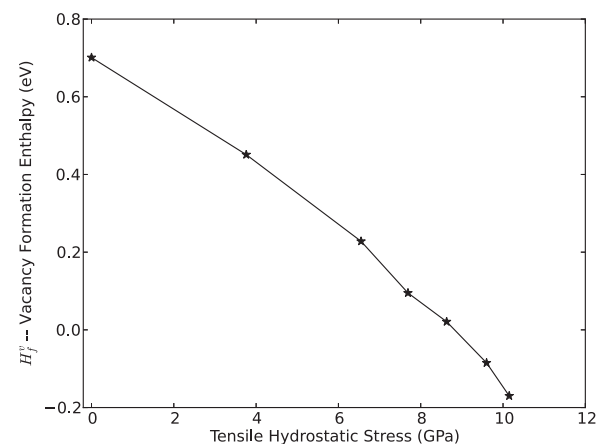


FIG. 2. Influence of hydrostatic stress on the formation enthalpy of a monovacancy in fcc aluminum.

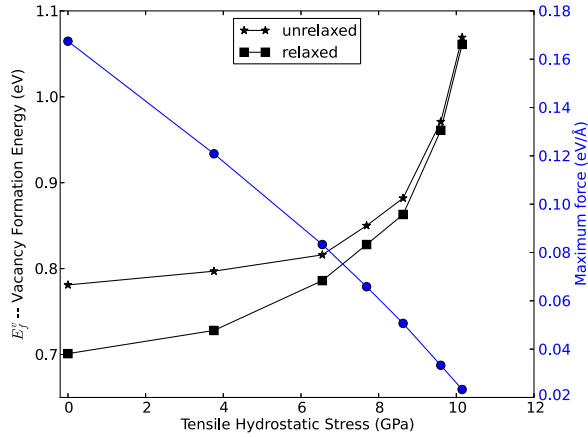


FIG. 3. (Color online) (Left axis) Formation energy of a monovacancy as a function of hydrostatic stress for the unrelaxed case (defect core energy) and the relaxed case. (Right axis) The maximum force experienced by atoms due to the perturbations in electronic structure created by the monovacancy.

state—and  $E_f$  denotes the formation energy. The contribution  $\sigma_0 V_f(\sigma_0)$  to the formation enthalpy is elastic in nature. On the other hand,  $E_f$  accounts for the effects of both the electronic structure and elastic interactions. The formation energy of a monovacancy at a given hydrostatic stress is given by

$$E_f^v(\sigma_0) = E(N-1, 1v, \sigma_0) - \frac{N-1}{N} E(N, 0, \sigma_0), \quad (2)$$

where  $E(N-1, 1v, \sigma_0)$  denotes the internal energy of a system comprising of  $N-1$  atoms and one vacancy computed at a hydrostatic stress  $\sigma_0$ , and  $E(N, 0, \sigma_0)$  denotes the energy of a perfect crystal containing  $N$  atoms at the same stress state. In order to delineate the contributions from the electronic structure and elastic interactions to the monovacancy formation energy, we conduct two sets of simulations: (i) suppressing the internal atomic relaxations and (ii) allowing for internal atomic relaxations. In the case where internal atomic relaxations are suppressed, the contribution to the formation energy is solely from the electronic structure, and represents the defect core energy. Figure 3 shows the formation energy of a monovacancy in the unrelaxed case (defect core energy) and the relaxed case as a function of hydrostatic stress. It is interesting to note that the defect core energy significantly changes with applied hydrostatic stress—from 0.78 eV at no hydrostatic stress to 1.07 eV at 10.15 GPa—and increases monotonically with the applied hydrostatic stress. Furthermore, we note that the contribution of elastic relaxations to the formation energy is small compared to the defect core energy—0.08 eV at no hydrostatic stress and monotonically reduces to 0.01 eV at 10.15 GPa. The monotonic decrease in the elastic relaxations is a result of the monotonic decrease in the forces experienced by the atoms due to the perturbations in electronic structure created by the vacancy. Figure 3 also shows that the maximum force experienced by the atoms, which is representative of the electronic structure at the defect core, changes by an order of magnitude for the range of hydrostatic stresses considered. The present results indicate that the electronic structure at the defect core changes significantly with the applied hydrostatic stress. Furthermore, we note that the change in the defect core energy

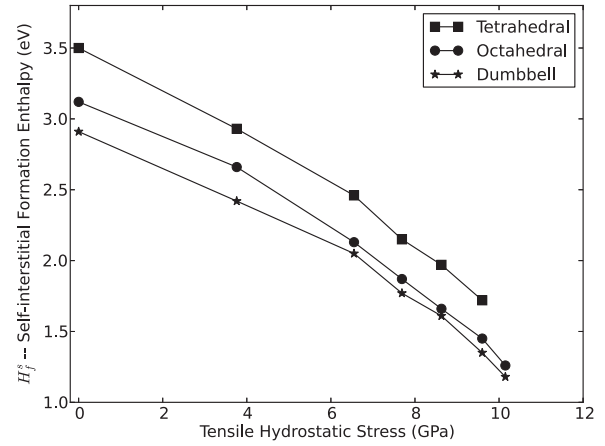


FIG. 4. Influence of hydrostatic stress on the formation enthalpy of tetrahedral, octahedral, and dumbbell self-interstitials in fcc aluminum.

over the range of hydrostatic stresses represents a significant fraction ( $\sim 1/3$ ) of the overall change in the formation enthalpy. These results underscore the importance of accounting for the defect core energy in the energetics of point defects, especially in the regime of extreme tensile stresses that are present in shocked metals.

We next study the influence of hydrostatic stress on the energetics of self-interstitials. We consider the three types of self-interstitials possible in fcc metals, which include the tetrahedral, the octahedral, and the dumbbell interstitial. The formation enthalpy of a self-interstitial is given by

$$H_f^s(\sigma_0) = H(N, 1s, \sigma_0) - \frac{N+1}{N} H(N, 0, \sigma_0), \quad (3)$$

where  $H(N, 1s, \sigma_0)$  denotes the enthalpy of a system comprising of  $N$  atoms and one self-interstitial atom at an interstitial site under an applied macroscopic hydrostatic stress  $\sigma_0$ . Figure 4 shows the formation enthalpy as a function of hydrostatic stress for tetrahedral, octahedral, and dumbbell self-interstitials. As in the case of monovacancy, the formation enthalpy of these point defects is significantly influenced by hydrostatic stress. In particular, the formation enthalpies monotonically decrease with increasing hydrostatic stress, and the change is  $\sim 1.7$  eV over the range of stresses considered in the present study. We also note that the dumbbell configuration is the most stable for the entire range of hydrostatic stresses considered in this study, however, the formation enthalpies of the octahedral self-interstitial are very close to that of the dumbbell self-interstitial for hydrostatic stresses greater than 6 GPa.

It is interesting to note that, while the formation enthalpies of the self-interstitials are positive for the range of tensile hydrostatic stresses considered, the formation enthalpy of a monovacancy changes sign and becomes negative for hydrostatic stresses beyond 9 GPa. This result has important implications on understanding the origins of spall failure in metals exposed to shock loading. Studies show that one possible mechanism of spall failure occurs through void nucleation and growth [30–32] under tensile hydrostatic stress, which in turn is mediated through vacancy coalescence

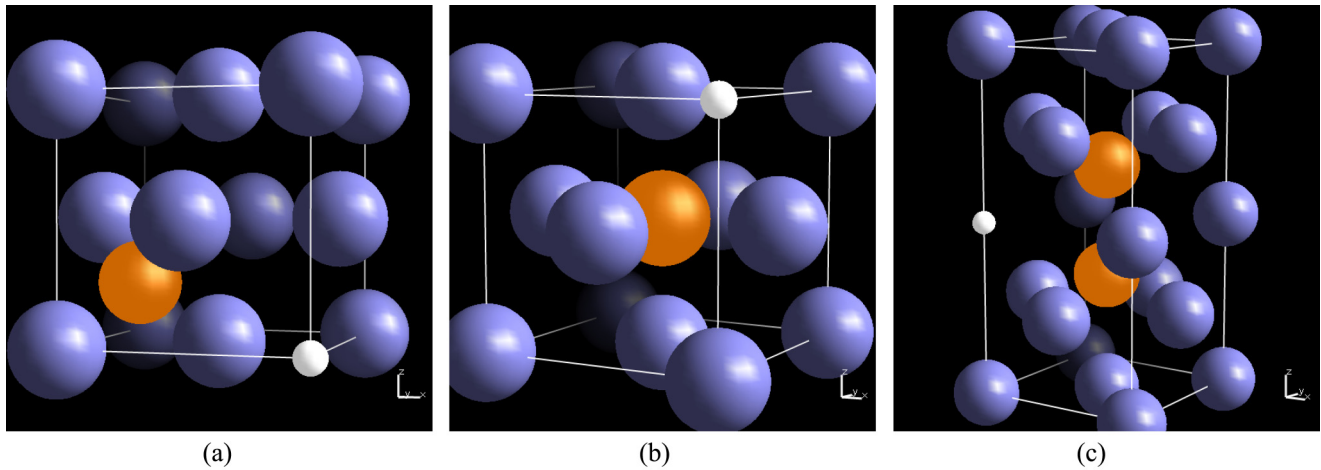


FIG. 5. (Color online) Schematics of stable Frenkel pairs considered in this work. Aluminum atoms occupying lattice sites are colored in blue, while aluminum atoms occupying interstitial positions are colored in orange. Vacancy sites are represented by small white spheres. (a) Tetrahedral Frenkel pair with the vacancy at the second nearest neighbor; (b) octahedral Frenkel pair with vacancy at the second nearest neighbor; and (c) dumbbell Frenkel pair with vacancy at third nearest neighbor.

[10]. However, the mechanisms of vacancy nucleation under shock loading have been elusive thus far. While entropic effects certainly play a role in vacancy nucleation at the high temperatures prevalent in shocked metals, the present results suggest that the effect of mechanical stresses on the energetics of vacancies is equally important. In particular, our study suggests that a spontaneous nucleation of vacancies is possible at hydrostatic stresses beyond the critical stress of 9 GPa, and represents a mechanical instability in the material, where the system prefers to nucleate a vacancy as opposed to accommodating a macroscopically affine deformation on a perfect crystal. We note that at finite temperatures, even below this critical stress, activated mechanisms can result in the nucleation of vacancies. As the formation enthalpy of monovacancy decreases with increasing hydrostatic stress, these results also suggest that it becomes increasingly easier for vacancies to nucleate with increasing hydrostatic stress, and provide a possible explanation for the nucleation of a large concentration of vacancies prior to void formation under shock loading.

However, since vacancies cannot nucleate in isolation, such a nucleation mechanism is only feasible at vacancy sources—like grain boundaries and dislocation cores—and represents a heterogeneous nucleation mechanism. Furthermore, a spall failure mediated through vacancy coalescence involves diffusive time scales and is a feasible mechanism for spalling at strain rates of  $\sim 10^4$ – $10^7$  s $^{-1}$ . However, experimental studies using ultrashort laser pulses ( $\sim 100$  fs) [33–35] with strain rates reaching  $10^8$  s $^{-1}$  and beyond also observe spall-like failure in metals, which suggests an alternate failure mechanism due to the very short time scales over which failure occurs that cannot support a diffusion limited failure mechanism. Moreover, experimental investigations also revealed a significant dependence of the spall strength on strain rates [36], especially for strain rates of  $10^8$  s $^{-1}$  and beyond, which also suggests the possibility of alternate mechanisms at high strain rates and short time scales.

To this end we study the feasibility of another possible failure mechanism through the formation of a Frenkel pair—

which constitutes a vacancy and self-interstitial pair in close proximity. We considered various Frenkel pairs formed from tetrahedral, octahedral, and dumbbell self-interstitials with the vacancy located at the nearest and second nearest lattice site. In the case of Frenkel pairs formed from tetrahedral and octahedral interstitials, for the range of hydrostatic stresses considered, the vacancy at the nearest neighbor recombined with self-interstitials, whereas the vacancy located at the second nearest lattice site was found to be stable. In the case of the Frenkel pair formed from the dumbbell self-interstitial, a vacancy at both the nearest and second nearest neighbor recombined, whereas the vacancy at the third nearest neighbor was found to be stable. Figure 5 shows the schematics for the stable Frenkel pair configurations. The computed formation enthalpy for these stable Frenkel pairs—the excess enthalpy

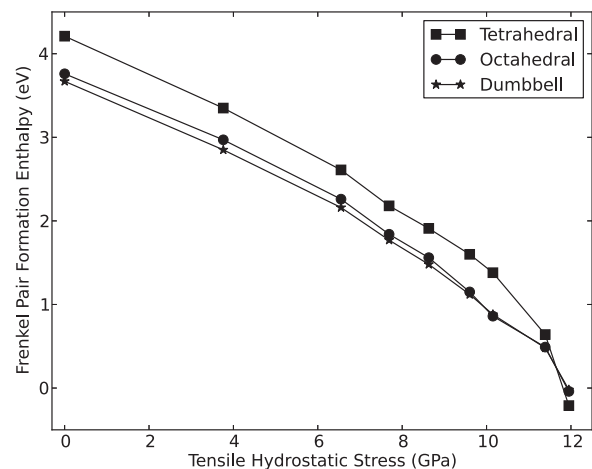


FIG. 6. Influence of hydrostatic stress on the formation enthalpy of stable Frenkel pairs in fcc aluminum comprising of: (i) a tetrahedral interstitial with vacancy at the second nearest lattice site; (ii) an octahedral interstitial with vacancy at the second nearest lattice site; and (iii) a dumbbell interstitial with vacancy at the third nearest lattice site (cf. Fig. 5 for schematics).

of the Frenkel pair measured with respect to a perfect crystal at the same stress state—as a function of hydrostatic stress is shown in Fig. 6. It is interesting to note that the formation enthalpy, as in the case of monovacancy and self-interstitials, monotonically decreases with increasing hydrostatic stress. Importantly, the formation enthalpy for these Frenkel pairs is negative for hydrostatic stresses close to 12 GPa, suggesting that a spontaneous nucleation of these defects is favorable at these hydrostatic stresses. We note that at this critical stress of 12 GPa the bulk modulus is computed to be 15.4 GPa, which implies that the crystal is sufficiently far from the stability limit and that the nucleation of Frenkel pairs is a possible failure mechanism prior to loss of crystal stability. The nucleation of Frenkel pairs constitutes a homogeneous nucleation mechanism, as these defects can nucleate from a perfect crystal and do not require any sources for their nucleation, and is a possible nucleation mechanism leading to spall failure in materials exposed to ultrashort time-scale (fs) shocks.

#### IV. SUMMARY

To conclude, we find a strong influence of macroscopic hydrostatic stresses on the energetics of point defects in aluminum, which include vacancies, self-interstitials, and Frenkel pairs. Importantly, we find that the defect core energy, which is governed by quantum-mechanical interactions at the core, is significantly influenced by the state of stress and plays an important role in governing the overall energetics of point defects. Our study suggests that the formation enthalpies of all point defects monotonically decrease with increasing hydrostatic

stress. In particular, the formation enthalpy of a monovacancy becomes negative for hydrostatic stresses greater than 9 GPa and the formation enthalpies of Frenkel pairs become negative for hydrostatic stresses of 12 GPa, which have important implications to nucleation mechanisms resulting in spall failure of metals exposed to shocks. These results suggest that spontaneous nucleation of vacancies from vacancy sources can mediate a heterogeneous nucleation of voids from vacancy coalescence leading to spall failure. However, in ultrafast shocks, where the time scales are too short for diffusion-limited vacancy coalescence, a homogeneous nucleation of Frenkel pairs can be a possible nucleation mechanism leading to spall failure at higher hydrostatic stresses.

#### ACKNOWLEDGMENTS

We gratefully acknowledge the support of the Air Force Office of Scientific Research under Grant No. FA9550-13-1-0113. V.G. gratefully acknowledges the Alexander von Humboldt Foundation through a research fellowship, and is grateful to the hospitality of the Institute of Applied Mechanics at University of Stuttgart while completing this work. T.M.P. gratefully acknowledges the support of the Office of Naval Research through Grant No. N00014-11-1-0616. This work, in part, used the Extreme Science and Engineering Discovery Environment (XSEDE), which is supported by National Science Foundation Grant No. OCI-1053575. We also gratefully acknowledge Advanced Research Computing at University of Michigan for providing the computing resources through the Flux computing platform.

- 
- [1] T. Mitchell, P. Peralta, and J. Hirth, *Acta Mater.* **47**, 3687 (1999).
  - [2] G. Lu and E. Kaxiras, *Phys. Rev. Lett.* **89**, 105501 (2002).
  - [3] M. Kabir, T. T. Lau, D. Rodney, S. Yip, and K. J. Van Vliet, *Phys. Rev. Lett.* **105**, 095501 (2010).
  - [4] A. V. der Ven, H.-C. Yu, G. Ceder, and K. Thornton, *Prog. Mater. Sci.* **55**, 61 (2010).
  - [5] Y. Shimizu, M. Uematsu, and K. M. Itoh, *Phys. Rev. Lett.* **98**, 095901 (2007).
  - [6] D. J. Bacon and T. D. de la Rubia, *J. Nucl. Mater.* **216**, 275 (1994).
  - [7] D. Bacon, Y. Osetsky, R. Stoller, and R. Voskoboynikov, *J. Nucl. Mater.* **323**, 152 (2003).
  - [8] B. D. Wirth, *Science* **318**, 923 (2007).
  - [9] V. Gavini, K. Bhattacharya, and M. Ortiz, *Phys. Rev. B* **76**, 180101 (2007).
  - [10] C. Reina, J. Marian, and M. Ortiz, *Phys. Rev. B* **84**, 104117 (2011).
  - [11] N. Chetty, M. Weinert, T. S. Rahman, and J. W. Davenport, *Phys. Rev. B* **52**, 6313 (1995).
  - [12] D. E. Turner, Z. Z. Zhu, C. T. Chan, and K. M. Ho, *Phys. Rev. B* **55**, 13842 (1997).
  - [13] Y. A. Wang, N. Govind, and E. A. Carter, *Phys. Rev. B* **60**, 16350 (1999).
  - [14] T. Uesugi, M. Kohyama, and K. Higashi, *Phys. Rev. B* **68**, 184103 (2003).
  - [15] G. Ho, M. T. Ong, K. J. Caspersen, and E. A. Carter, *Phys. Chem. Chem. Phys.* **9**, 4951 (2007).
  - [16] V. Gavini, *Phys. Rev. Lett.* **101**, 205503 (2008).
  - [17] P. Olsson, T. P. C. Klaver, and C. Domain, *Phys. Rev. B* **81**, 054102 (2010).
  - [18] V. Gavini, *Proc. R. Soc. A* **465**, 3239 (2009).
  - [19] Z. Chen, N. Kioussis, N. Ghoniem, and D. Seif, *Phys. Rev. B* **81**, 094102 (2010).
  - [20] M. J. Aziz, *Appl. Phys. Lett.* **70**, 2810 (1997).
  - [21] K. Garikipati, M. Falk, M. Bouville, B. Puchala, and H. Narayanan, *J. Mech. Phys. Solids* **54**, 1929 (2006).
  - [22] X. Gonze, B. Amadon, P.-M. Anglade, J.-M. Beuken, F. Bottin, P. Boulanger, F. Bruneval, D. Caliste, R. Caracas, M. Cote *et al.*, *Comput. Phys. Commun.* **180**, 2582 (2009).
  - [23] M. Torrent, F. Jollet, F. Bottin, G. Zérah, and X. Gonze, *Comput. Mater. Sci.* **42**, 337 (2008).
  - [24] J. P. Perdew and A. Zunger, *Phys. Rev. B* **23**, 5048 (1981).
  - [25] P. E. Blöchl, *Phys. Rev. B* **50**, 17953 (1994).
  - [26] N. Holzwarth, A. Tackett, and G. Matthews, *Comput. Phys. Commun.* **135**, 329 (2001).
  - [27] H. J. Monkhorst and J. D. Pack, *Phys. Rev. B* **13**, 5188 (1976).

- [28] V. Gavini, K. Bhattacharya, and M. Ortiz, *J. Mech. Phys. Solids* **55**, 697 (2007).
- [29] B. Radhakrishnan and V. Gavini, *Phys. Rev. B* **82**, 094117 (2010).
- [30] E. T. Seppälä, J. Belak, and R. E. Rudd, *Phys. Rev. B* **69**, 134101 (2004).
- [31] E. T. Seppälä, J. Belak, and R. E. Rudd, *Phys. Rev. Lett.* **93**, 245503 (2004).
- [32] J. Marian, J. Knap, and M. Ortiz, *Phys. Rev. Lett.* **93**, 165503 (2004).
- [33] H. Tamura, T. Kohama, K. Kondo, and M. Yoshida, *J. Appl. Phys.* **89**, 3520 (2001).
- [34] J. P. McDonald, S. Ma, T. M. Pollock, S. M. Yalisove, and J. A. Nees, *J. Appl. Phys.* **103**, 093111 (2008).
- [35] B. J. Demaske, V. V. Zhakhovsky, N. A. Inogamov, and I. I. Oleynik, *Phys. Rev. B* **82**, 064113 (2010).
- [36] E. Moshe, S. Eliezer, Z. Henis, M. Werdiger, E. Dekel, Y. Horovitz, S. Maman, I. B. Goldberg, and D. Eliezer, *Appl. Phys. Lett.* **76**, 1555 (2000).